Landscape evolution and pattern formation: modeling, analysis and simulation

par

Julie Binard, Pierre Degond, Pascal Noble

Institut de Mathématiques de Toulouse, INSA Toulouse, CNRS

Mini-Symposium La mécanique des fluides dans tous ses états

Outline

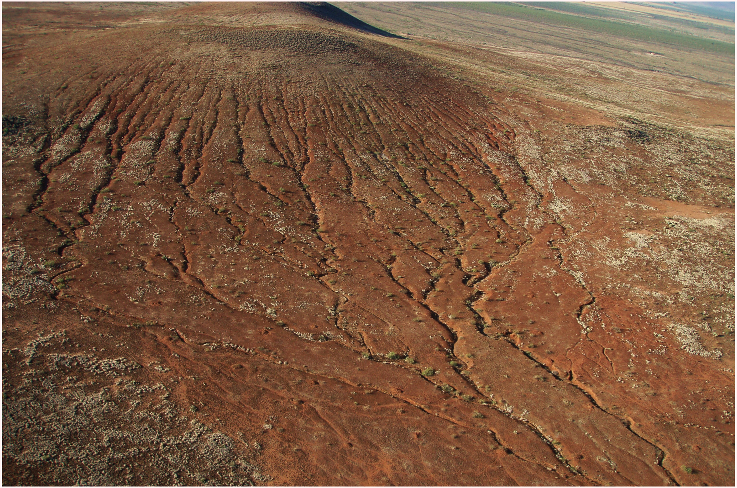

Figure: A drainage pattern in the San Simon Valley in New Mexico [1].

[1] https://www.flickr.com/photos/balvarius/3662158543/

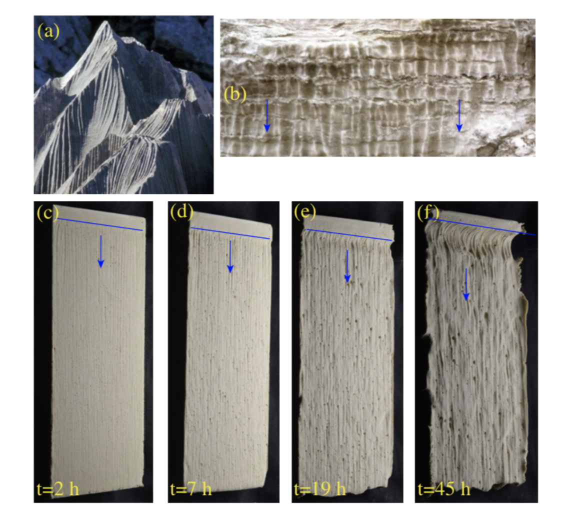

Figure: Fig (a): Dissolution rills on limestone (Karst Plateau, Slovenia). Fig (b): Rills on gypsum (Vaucluse, France), Fig (c-f): Experimental dissolution pattern on gypsum.

2

[2] A. Guérin et al, Phys Rev Letters 125 (2020)

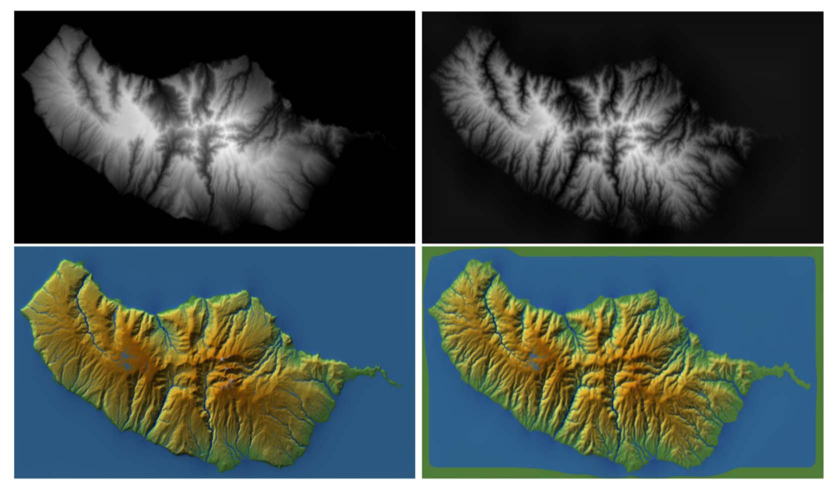

Figure: Numerical Simulation of an evolution landscape (Madeira). Top: Evolution of channels. Bottom: Topographic renderings

[3]

[3] Lebrun et al, Image Proc Online 8 (2018)

1. Physical mechanism of their formation: Influence of rainfalls? Dissolution ? Sedimentation ?

2. What does set the scale of the patterns? How does evolve drainage areas?

3. More: What does the morphology of the patterns tell about past history? Erosion rate? Age of exposure ?

Outline

1. Erosion (of rocks, soils,): fluid (water, snow, air) strain on the landscape, chemical reaction (dilution), extreme events (landslides, avalanches)
2. Transport of sediments (solid or diluted) with two types of regimes:
   - A. "transport limited" regime (sediments easily transport like sand, muds in rivers),
   - B. "detachment limited" regime (rivers in mountains do not carry much sediments and water hollows rocks).
3. Sediments deposition, debris accumulation
4. Other effects: creeping, tectonic uplift, lava flow,...

Topography evolution: Creep effect

- The creep effect: the soil is subject to a diffusion process, which tends to smooth the surface.
- Creep is due to multiples processes, that act under the constraint of gravity: Wind, rain, splash, Expansions and contractions of the soil due to freeze-thaw, wet-dry and hot-cold cycles, Biological activity...
- This term plays a significant role in the formation of patterns.

Figure: Terracettes in WiltShire, England [4].

[4] Author: Derek Harper

LEM

$$\begin{cases} \partial_t h + \operatorname{div}(h\mathbf{v}) = r, & \text{Equation on fluid height} \\ \partial_t(ch) + \operatorname{div}(ch\mathbf{v}) = \rho_s e h^m |\mathbf{v}|^n - \rho_s sc, & \text{Equation on concentration} \\ \partial_t z = K\Delta z + sc - eh^m|\mathbf{v}|^n, & \text{Equation on surface height} \end{cases} \quad (1)$$

where the water speed is given by $\mathbf{v} = -V_{ref}\nabla(h+z)$.

Theorem (Binard, Degond, N): Local Well-Posedness

Let $m > 0$, $n > 3$ or $n = 2$, $K > 0$, and $T_0 > 0$. Let us fix two constants fluid heights $h_{ref} > h_{min} > 0$. Suppose that the initial data h^0, z^0, c^0 satisfy

$$h^0 - h_{ref},\, z^0 \in H^{k+1}(\mathbb{R}^2), \quad c^0 \in H^k(\mathbb{R}^2), \quad h^0(x) \geq 2\,h_{min}\,\forall x \in \mathbb{R}^2.$$

with $k = 3$. Suppose that $r \in L^2_{T_0}(H^k)$, $K\,h_{min} - ||h^0||^2_{L^\infty} \geq 0$. Then there exists $0 < T < T_0$ such that **System (1) admits a unique solution** (h, z, c) **with**

$$h - h_{ref},\, z \in L^2_T(H^{k+2}) \cap C_T(H^{k+1}), \quad c \in C_T(H^k).$$

A simplified model (by Bonetti et al, PNAS 117 (2020) no 3)

$$-\mathrm{div}\left(hV_0\frac{\nabla z}{|\nabla z|}\right)=R,\quad \partial_t z = K\Delta z - eh^m|\nabla z|^n + U$$

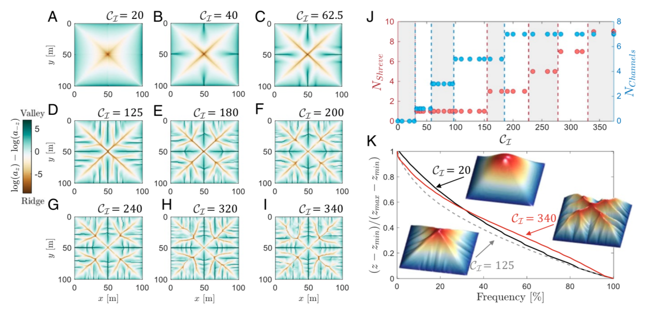

FIGURE: Channelization Cascade in a simplified LEM (no sediment, uplift): the channelization index $\mathcal{C}_\mathcal{I}$ increases as $K \to 0$

- What about channelization in tilted plane? Transverse instabilities?

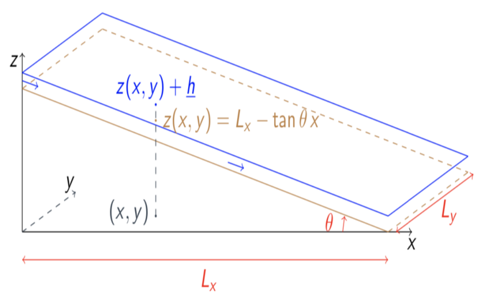

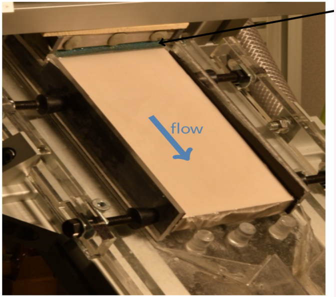

- Fluid is flowing down a tilted plane. Fluid height and velocity are constant.

- $\underline{\mathbf{v}}(t,x,y) = -\tan\theta\, e_1, \quad \underline{c}(t,x,y) = \frac{e}{s}\underline{h}^m|\underline{\mathbf{v}}|^n.$

1. **Case $K > 0$**

   - There exists a constant $\gamma > 0$ independent of n such that the system is spectrally **stable at all frequencies** $(\xi, \eta) \in \mathbb{R}^2_*$ if and only if

     $$K \geq m\underline{hc}\frac{e}{V} := \bar{K} \quad \text{and} \quad n < \gamma.$$

     Proof by Routh-Hurwitz stability criterion.

   - Creeping has a stabilising effect on the system.

2. **Case $K = 0$**

   - If $K = 0$, the system is **spectrally unstable**. The wave associated to the wavevector (ξ, η) is stable if and only if

     $$m\underline{c} < 1 \quad \text{and} \quad \eta^2 m < \xi^2(n - m).$$

   - High frequencies are unstable.
     - (A) If $n \leq m$ then the system is unstable at all frequencies.
     - (B) If $n \geq m$, the system is unstable in the transverse direction ($\xi = 0$). This may lead to the formation of rills in the direction of the water flux.

In the unstable regime $0 < K < \bar{K}$, we can precise the instability scenarii. The unstable domain is always bounded.

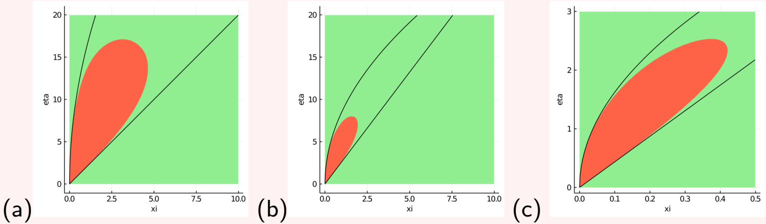

FIGURE: (a) $K = 0.6m\underline{hc}e/V$, (b) $K = 0.75m\underline{hc}e/V$, (c) $K = 0.9m\underline{hc}e/V$.

The black curves are boundary between stable and unstable areas, calculated at low frequencies.

Outline

- **Framework:** we considered the characteristic velocities in the experiment by Derr et al: erosion rate $0.1mm/h$, fluid velocity $0.1m/s$, fluid height, variation of topography: $0.1mm$, $2-5mm$
- Write the LEM with non dimensional variables:

$$\begin{cases} \varepsilon\partial_t h + \mathrm{div}(h\mathbf{v}) = r, \\ \varepsilon\partial_t(ch) + \mathrm{div}(ch\mathbf{v}) = h^m|\mathbf{v}|^n - \sigma c, \\ \partial_t z = \kappa\Delta z - h^m|\mathbf{v}|^n + \sigma c, \end{cases}$$

where $\varepsilon = \dfrac{e}{V} \ll 1$, $\kappa = \dfrac{K}{eZ}$, $\sigma = \dfrac{s}{e}$

- Numerical simulations of the full system introduces very restrictive CFL.
- We consider the asymptotic model:

$$\begin{cases} \mathrm{div}(hv) = r, \\ \mathrm{div}(chv) = eh^m|\mathbf{v}|^n - \sigma c, \\ \partial_t z = \kappa\Delta z - eh^m|\mathbf{v}|^n + \sigma c. \end{cases}$$

- We can choose bigger time steps for the numerical simulations, and solve the two first equations at each time step of the last equation.
- In practice, simulations of the non stationary system, and of the stationary system give the same results.

- Equation on $h^{k+1} \approx h(t_{k+1}, .)$ is solved by a finite volume scheme.

$$-\mathrm{div}(h^k \nabla h^{k+1}) - \mathrm{div}(h^{k+1} \nabla z^{k+1}) = r^{k+1}.$$

- Equation on c^{k+1} is solved by a finite volume scheme, seeing x as a time variable.

$$\partial_x c^{k+1} + \frac{\partial_y (h^{k+1} + z^{k+1})}{\partial_x (h^{k+1} + z_{k+1})} \partial_y c^{k+1} = -\frac{(h^{k+1})^m |\mathbf{v}^{k+1}|^n - \sigma c^{k+1} - r^{k+1}}{h^{k+1} \partial_x (h^{k+1} + zk + 1)}.$$

- Equation on z is solved with an explicit Euler scheme.

$$z^{k+1} = z^k + dt \left(\kappa \Delta z^k - e(h^k)^m |\mathbf{v}^k|^n + \sigma c^k \right)$$

- Boundary conditions:
  1. periodic in the transverse variable y,
  2. At $x = 0$, prescribed water height h_0, concentration c_0
  3. At $x = L$, Neumann boundary conditions, no flux

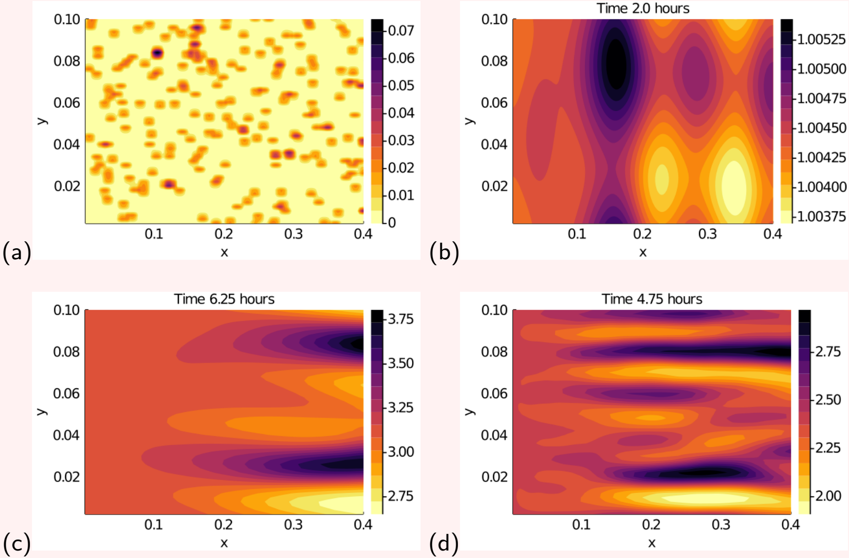

FIGURE: From top left to bottom right: (a) initial surface; final surface for: (b) $K = K_e$; (c) $K = K_e/20$; (d) $K = K_e/50$

Conclusions

1. Local well-posedness for LEM under the restriction that the **fluid height does not vanish**
2. Spectral stability results show that the creep effect plays a significant role: small creep (large channelization index) promotes instabilities in particular transverse instabilities
3. Numerical simulations with finite volume methods confirm the instability scenarii

Limitations

1. Dry areas appear on large time simulations and numerical instabilities occur
2. Existence of solutions on (arbitrary) large time: dealing also with dry areas (no control on the minimum fluid height)
3. Understanding of channelization: introduction of randomness

Idea: we introduce randomness in the process of (micro)-channel creation through a Poisson process with parameter $\mu(x,t)$

- The probability of creating k canals during the time interval $[t, t+\delta t]$ and in a domain B is

$$\frac{\left(\int_B \int_t^{t+\delta t} \mu(s,y)dsdy\right)^k}{k!} \exp\left(-\int_B \int_t^{t+\delta t} \mu(s,y)dsdy\right),$$

$$\mu(t,x) = e\left(\frac{h(t,x)}{H}\right)^m \left(\frac{|\mathbf{v}(t,x)|}{V}\right)^n.$$

- Probability that one channel is created: $1 - \exp\left(-\int_B \int_t^{t+\delta t} \mu(s,y)dsdy\right)$.
- We denote $\Gamma_i(x)$ the shape of the i-th channel et t_i the time it is created

$$\partial_t z = K\Delta z - \sum_{i=1}^{n(T)} \Gamma_i(x)\delta_{t_i}(t).$$

- Shape of the channel $\Gamma_i(x) = f\left(\langle x - x_i, \omega\rangle, \langle x - x_i, \omega\rangle\right)$ with $\omega \in \mathbb{S}^1$ chosen with the Van Mises law

$$\frac{1}{Z(\kappa)} e^{-\kappa\langle\omega, \frac{\mathbf{v}}{|\mathbf{v}|}\rangle}, \quad Z(\kappa) = \int_0^{2\pi} e^{-\kappa\cos(\theta)}d\theta.$$

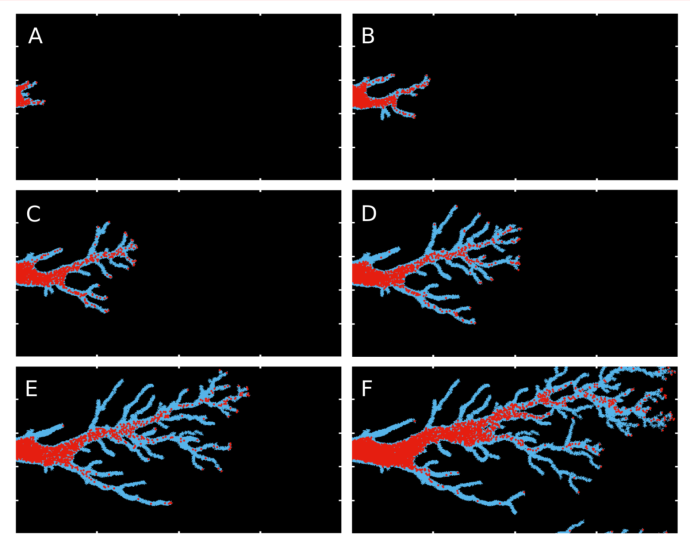

Figure: Emergence of blood capillary networks in tissue[5]

[5] Aceves-Sanchez et al, arXiv 2018

- Dealing with dry areas is hardly treated with finite volume schemes, in particular with degenerate viscosity.
- SPH (Smoothed Particle Hydrodynamics) are well suited for dry areas: the solution is approximated by a sum of (smoothed) Dirac.
- Main issue: equations on (h, c) are stationnary and SPH methods need an adaptation to this framework.

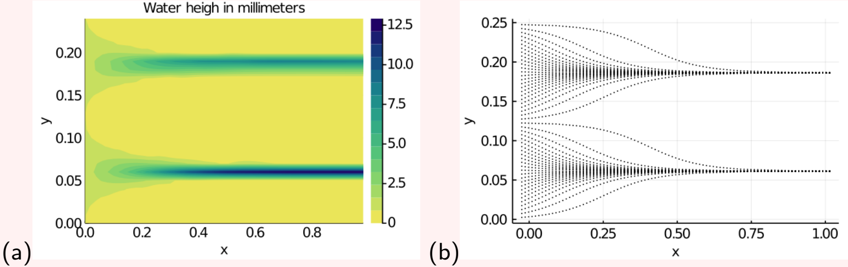

Figure: (a) Water height, on the domain Ω (b)Particle positions, on the domain Ω.